

Electronic structure of phthalocyanines: Theoretical investigation of the optical properties of phthalocyanine monomers, dimers, and crystals

E. Ortí^{a)} and J. L. Brédas

Service de Chimie des Matériaux Nouveaux, Département des Matériaux et Procédés, Université de Mons, B-7000 Mons, Belgium

C. Clarisse

Centre National d'Etudes des Télécommunications, Route de Trégastel-BP 40, F-22301 Lannion, France

(Received 14 July 1989, accepted 12 October 1989)

We present valence effective Hamiltonian (VEH) calculations on the optical absorptions of a series of phthalocyanine compounds: the metal-free phthalocyanine molecule, a model system for the lithium phthalocyanine molecule, the metal-free phthalocyanine dimer, and model systems for the lutetium diphthalocyanine and the lithium phthalocyanine crystal. For these compounds, it is found that the major factor influencing the evolution of the optical transitions is not the electronic structure of the metal but rather the geometric structure: phthalocyanine intraring geometry and, in the dimers and crystals, interring separation and staggering angle. The origin of the so-called Soret or *B* absorption band is calculated to be significantly more complex than was previously thought on the basis of the simple four-orbital model.

I. INTRODUCTION

Phthalocyanine (Pc) compounds have attracted a great deal of attention for a long time because of their unique properties such as semiconductivity, photoconductivity, and chemical activity.¹ (For instance, Vartanyan² measured the photoconductivity of the different α and β polymorphic forms of phthalocyanines as early as 1948.) Besides their excellent photoconductive properties, phthalocyanines have the advantage of being very stable against thermal and chemical decomposition and present very intense optical absorptions in the visible. These properties, together with the structural similarity to chlorophyll, has resulted in many investigations toward their application in artificial solar energy conversion.¹ Also, they are expected to serve as active materials for molecular electronic devices such as electrochromic displays and chemical sensors.³ Furthermore, interest in phthalocyanine compounds has recently been renewed due to the discovery that they form "molecular metals" after partial oxidation.⁴ While crystals of pure phthalocyanine exhibit conductivities (σ) in the insulating range ($\sigma < 10^{-10}$ S/cm),⁵ iodine oxidized crystals show conductivities on the order of 10–1000 S/cm at room temperature.⁴

In a recent work,⁶ we have analyzed in great detail, on the basis of valence effective Hamiltonian calculations, the ultraviolet and x-ray photoemission spectroscopy (UPS and XPS, respectively) data reported on metal-free phthalocyanine.^{7,8} The excellent quantitative agreement obtained between theory and experiment allowed us to provide an unambiguous interpretation of all the valence electronic features observed experimentally. It also illustrated the validity of the valence effective Hamiltonian (VEH) approach to study the electronic structure of macrocycles such as phthalocyanine.

In the present paper, we focus on the optical properties

and compare the optical absorption data for three sets of phthalocyanine compounds:

- (i) monomeric systems: metal-free phthalocyanine (PcH₂) and lithium phthalocyanine (PcLi);
- (ii) dimeric compounds: metal-free phthalocyanine dimer (PcH₂)₂ and lutetium diphthalocyanine (Pc₂Lu);
- (iii) the PcLi crystal.

The relevance of Pc₂Lu and PcLi in the context of organic semiconductors is determined by the fact that they are claimed to be the first molecular semiconductors reported to date.^{9–11} (A molecular semiconductor is defined by André *et al.*^{9–12} as a molecular material, i.e., a material constituted of well-characterized molecular units, which exhibits an intrinsic conductivity in the range 10^{-6} – 10^{-1} S/cm and can be doped with both electron donors or acceptors.) Room temperature conductivities as high as 6×10^{-5} and 2×10^{-3} S/cm have been respectively measured for single crystals of Pc₂Lu¹³ and PcLi¹⁰ under vacuum to avoid any fortuitous external doping. These high conductivities are to be compared with those reported for single crystals of PcH₂,¹⁴ PcCu,¹⁵ or PcNi,¹⁶ all of which present values lower than 10^{-12} S/cm.

We have followed a methodology identical to that detailed earlier.⁶ All the calculations have been performed in the framework of the valence effective Hamiltonian (VEH) quantum-chemical technique. The VEH method has been originally developed for molecules¹⁷ and later extended for stereoregular polymers.^{18,19} The method takes only into account the valence electrons and is based on the use of an effective Fock Hamiltonian parameterized to reproduce the results of *ab initio* calculations. In this way, the VEH method is completely nonempirical and yields one-electron energy levels of Hartree–Fock *ab initio* double-zeta quality. All the calculations have been performed using the new parameterization recently obtained for the carbon and hydrogen atoms.²⁰ The VEH parameters used for nitrogen atoms are those previously reported.⁴

^{a)} Permanent address: Departamento de Química Física, Facultad de Química, Universidad de Valencia, Dr. Moliner, 50, 46100-Burjassot, Valencia, Spain.

The results are presented and discussed in Sec. II for the monomeric compounds, in Sec. III for the dimeric compounds, and in Sec. IV for the PcLi crystal. The main conclusions of our work are summarized in Sec. V.

II. MONOMERIC COMPOUNDS: METAL-FREE PHTHALOCYANINE AND LITHIUM PHTHALOCYANINE

The neutron diffraction structure reported by Hoskins *et al.*²² has been assumed as the input geometry for PcH₂. This structure attributes a planar C_{2h} geometry to the PcH₂ molecule and locates the central two hydrogens on opposite nitrogens. The calculations have been performed both on this C_{2h} geometry and on an averaged D_{2h} structure sketched in Fig. 1. Since both geometries lead to identical results, only the D_{2h} results are presented and discussed below.

Figure 2 displays the VEH one-electron energy level distribution obtained for PcH₂. Since 186 valence electrons are involved in PcH₂ molecule, the molecular orbital number 93 corresponds to the highest occupied molecular orbital (HOMO). This MO is of π type and has a_u symmetry with no contribution from the nitrogen atoms. Our assignment supports that obtained using PPP²³ and CNDO²⁴ semi-empirical methods and contrasts with that calculated with the more approximate extended Hückel²⁵ technique and the one-electron Hartree-Fock-Slater²⁶ method.

All the molecular orbitals displayed in Fig. 2 are of π type, the first occupied σ orbital lying at an energy of -10.38 eV. The 4a_u HOMO is located at -6.32 eV in very good agreement with the first ionization energy (6.41 eV) obtained from the gas-phase UPS spectrum of PcH₂.⁷ Note the important energy gap (3 eV) that separates this orbital from the 7b_{1u} MO heading the next set of occupied molecular orbitals. This gap is also in very good accord with experimental UPS data.⁷ (A detailed discussion of the valence electronic structure of PcH₂ is found in Ref. 6. The slight differences between the one-electron energies reported in

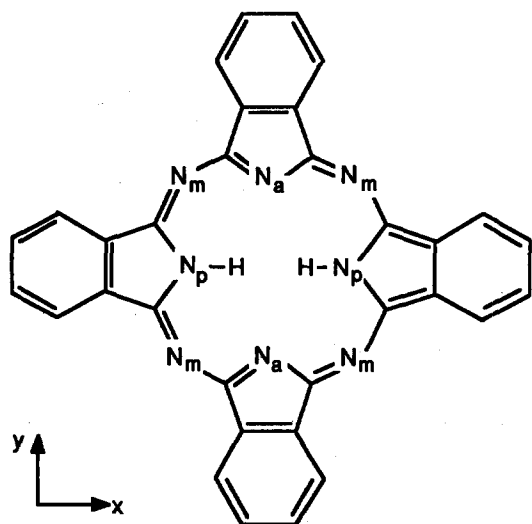


FIG. 1. Molecular structure of metal-free phthalocyanine. N_p denotes a pyrrole nitrogen and N_a and N_m denote pyrrole aza and mesobridging aza nitrogens, respectively.

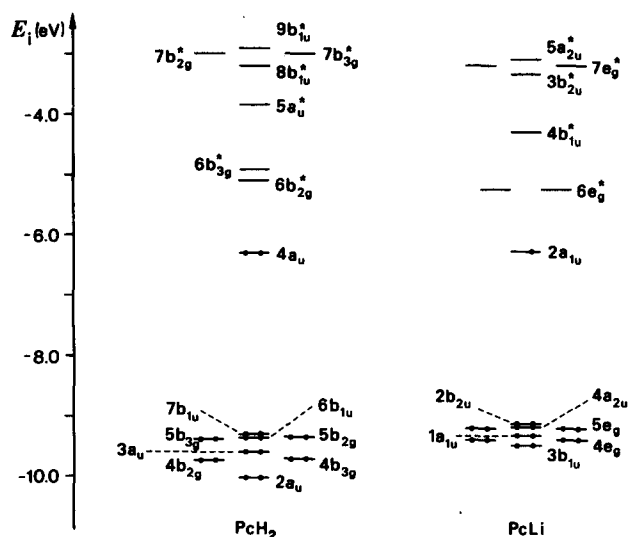


FIG. 2. VEH one-electron energies (E_i) and symmetries of the upper occupied and lower unoccupied molecular orbitals calculated for PcH₂ and the PcLi model system. All the orbitals are of π type.

that work and those presented here are due to the previous use of the old VEH parameterization for carbon and hydrogen atoms.¹⁹ In any case, the new parameterization used here does not affect the quantitative agreement with experimental data found in Ref. 6.)

The lowest unoccupied molecular orbital (LUMO) corresponds to the 6b_{2g} (π^*) molecular orbital in Fig. 2; it has nonzero coefficients on the pyrrole nitrogens (N_p in Fig. 1). The 6b_{3g} (π^*) molecular orbital is at higher energy and has nonzero coefficients on the pyrrole aza nitrogens (N_a in Fig. 1). The quasidegeneracy of these two orbitals (they are separated by only 0.17 eV) is due to the quasi-identical geometry of all the isoindole moieties. This feature implies that the carbon-nitrogen π -electron system effectively nearly possesses D_{4h} symmetry.

Turning to the optical spectrum, the energies and oscillator strengths calculated for the electronic transitions lower in energy than 4.5 eV (275 nm) are collected in Table I. Since the VEH method yields, as any other *ab initio* technique, too wide a valence electronic structure, a contraction of the energy scale for the occupied valence levels becomes necessary to obtain the best correlation with experimental data. (A contraction factor of 1.3 has been used as discussed in Ref. 6.) On the other hand, the VEH method predicts a HOMO-LUMO energy gap of only 1.22 eV, underestimating by 0.59 eV the energy of the first optical transition (1.81 eV) reported for the PcH₂ molecule.²⁷ Therefore, the energies in Table I represent one-electron energy differences obtained from the ground state levels depicted in Fig. 2 after a contraction of 1.3 of the occupied levels and a shift of 0.59 eV to higher energies of all the unoccupied levels. These adjustments are systematically used in all the other systems investigated in this work in order to provide a consistent picture and meaningful comparisons. (We must stress that the same approach has been used in works on other macrocycles with similar success.²⁸)

The theoretical data in Table I indicate the occurrence of two intense optical transitions in the visible at 1.81 eV

TABLE I. VEH electronic transitions calculated for PcH_2 and the PcLi model system. Transitions more energetic than 4.5 eV or with oscillator strengths lower than 0.1 are not included. Energies are in eV (nm in parentheses).

| | Transition | Energy ^a | Oscillator strength | Polarization ^b |
|------------------------------|---------------------------------|------------------------------|---------------------|---------------------------|
| PcH_2 | $4a_u \rightarrow 6b_{2g}^*$ | 1.81 (685) | 5.1 | y |
| | $4a_u \rightarrow 6b_{3g}^*$ | 1.98 (625) | 4.7 | x |
| | $4a_u \rightarrow 7b_{2g}^*$ | 3.90 (318) | 0.4 | y |
| | $4a_u \rightarrow 7b_{3g}^*$ | 3.91 (317) | 0.3 | x |
| | $7b_{1u} \rightarrow 6b_{2g}^*$ | 4.12 (301) | 1.6 | x |
| | $6b_{1u} \rightarrow 6b_{2g}^*$ | 4.15 (299) | 0.3 | x |
| | $7b_{1u} \rightarrow 6b_{3g}^*$ | 4.29 (289) | 1.6 | y |
| | $6b_{1u} \rightarrow 6b_{3g}^*$ | 4.32 (287) | 0.3 | y |
| | $3a_u \rightarrow 6b_{2g}^*$ | 4.38 (283) | 1.2 | y |
| | PcLi | $2a_{1u} \rightarrow 6e_g^*$ | 1.62 (764) | 5.6 |
| $5e_g \rightarrow 2a_{1u}$ | | 2.30 (538) | 1.2 | x,y |
| $4e_g \rightarrow 2a_{1u}$ | | 2.42 (512) | 1.6 | x,y |
| $3e_g \rightarrow 2a_{1u}$ | | 3.01 (411) | 1.5 | x,y |
| $2b_{2u} \rightarrow 6e_g^*$ | | 3.91 (317) | 0.3 | x,y |
| $4a_{2u} \rightarrow 6e_g^*$ | | 3.92 (316) | 1.5 | x,y |
| $1a_{1u} \rightarrow 6e_g^*$ | | 3.98 (311) | 0.9 | x,y |
| $3b_{1u} \rightarrow 6e_g^*$ | | 4.05 (306) | 1.2 | x,y |

^a Transition energies are calculated as one-electron energy differences after a contraction of 1.3 of the occupied levels and a shift of 0.59 eV to higher energies of the unoccupied levels. (See the text for further details.)

^b Axes refer to those presented in Fig. 1.

(685 nm) and 1.98 eV (625 nm), respectively, and a set of less intense transitions in the near UV around 300 nm. These results are in very good agreement with the vapor absorption spectra reported by Edwards and Gouterman²⁷ for PcH_2 in the region of 145–2500 nm. The experimental data predict no electronic transition above 700 nm, two sharp peaks in the visible region at 686 nm (Q_x) and 622 nm (Q_y) (that constitute the so-called band Q), a less intense broad band centered at 340 nm (named Soret or B band), and other bands (N , L , and C) below 280 nm. Band Q in the visible can be clearly correlated with the $4a_u \rightarrow 6b_{2g}^*$ (1.81 eV) and $4a_u \rightarrow 6b_{3g}^*$ (1.98 eV) electronic transitions. Both the splitting of this band (0.18 eV) and the relative intensity of the constituent peaks (Q_x more intense than Q_y) are very well reproduced by the theoretical calculations. By general convention, the lower energy Q band is referred to as Q_x without implying any absolute orientation. The important fact is that, when adopting as x the axis defined by the central two hydrogens as depicted in Fig. 1, the lower energy Q_x band is calculated to be polarized following the y axis (see Table I), i.e., perpendicular to the H–H axis.

As can be observed from Table I, the next relevant theoretical transition corresponds to the $7b_{1u} \rightarrow 6b_{2g}^*$ excitation located at 4.12 eV. This transition is imbedded in a group of very close-lying transitions starting with the $4a_u \rightarrow 7b_{2g}^*$ excitation at 3.90 eV and which can be correlated with the

broad B band measured to be centered at 3.65 eV and to extend from 3.3 to 4.1 eV.²⁷ Although the VEH calculations overestimate the energy of the electronic transitions corresponding to band B , it must be taken into account that we are working in a single-configuration approach and important configuration interaction can be expected when electronic transitions of the same symmetry take place at similar energies. This configuration mixing can significantly affect the energy of the resulting excited states. It can be therefore concluded that the four orbital model proposed by Weiss *et al.*²⁹ is not valid to explain the origin of band B in PcH_2 since several electronic transitions are involved in this band and no clear theoretical assignment is possible. The complex nature of band B is supported by the magnetic circular dichroism spectra reported for PcH_2 .³⁰ These spectra suggest that there are at least three distinct states in region B arising from π -molecular orbitals.

Note that the four orbital model was originally introduced to study free base porphine (PH_2).²⁹ This model explains the origin of bands Q and B by only considering the highest two occupied MOs (a_u and b_{1u}) and the lowest two unoccupied MOs (b_{2g}^* and b_{3g}^*). Preliminary VEH calculations on PH_2 indicate that the $5b_{1u}$ MO is separated by only 0.5 eV from the $2a_u$ HOMO and by 2 eV from the rest of occupied orbitals in contrast to the situation found in PcH_2 .³¹ This feature indicates that no high configuration mixing can be expected between electronic transitions from the $5b_{1u}$ and lower energy levels. The four orbital model is therefore valid for PH_2 where band B results mainly from the $5b_{1u} \rightarrow b_g^*$ transitions, but cannot be extended for phthalocyanine.

The x-ray crystallographic structure reported by Sugimoto *et al.*³² has been adopted as input geometry for the PcLi molecule. It is very important to note that the VEH calculations have been performed on the phthalocyanine ring *without taking explicitly into account the lithium atom*. Justification of such an approach, where *the influence of the metal is exclusively considered through the Pc ring geometry modifications*, will become clear later on. The Li atom gives one electron to the Pc ring which becomes a stable monoanion radical (Pc^-). The resulting one-electron energy level distribution is displayed in Fig. 2 together with that of PcH_2 for the sake of comparison. Although the PcLi molecular geometry presents some significant distortions from planarity, it remains very close to a D_{4h} symmetry and molecular orbitals in Fig. 2 have been classified according to that symmetry group.

As can be seen from Fig. 2, the molecular orbital distribution of the PcLi model is very similar to that obtained for PcH_2 . The main difference between PcLi and PcH_2 is that for the former the $2a_{1u}$ HOMO is occupied by a single electron due to the radical nature of the phthalocyanine ring. It must also be noted that the quasidegeneracy of the $6b_{2g}^*$ and $6b_{3g}^*$ MOs in PcH_2 almost disappears in PcLi to give rise to the degenerate $6e_g^*$ MO. Moreover, the LUMO level is closer to the HOMO in PcLi than in PcH_2 by 0.19 eV. As a consequence of these features, additional electronic transitions between lower occupied levels and the $2a_{1u}$ HOMO take place in PcLi and the HOMO \rightarrow LUMO transition is no long-

er split into two peaks. The energies and oscillator strengths obtained for the electronic transitions of the PcLi molecule are summarized in Table I. The transition energies are calculated in the same way as discussed above for PcH_2 .

The experimental optical spectrum reported by Turek *et al.*³³ for PcLi in 1-chloronaphthalene solution shows well defined absorptions at 1.32 eV (940 nm), 1.53 eV (810 nm), 1.79 eV (690 nm), 2.62 eV (473 nm), 2.90 eV (427 nm), and 3.35 eV (370 nm). If we compare this spectrum with the theoretical transitions collected in Table I, we find the following features:

(i) The broad band near 1.32 eV and the band at 1.79 eV are assigned by the authors to aggregation phenomena and PcH_2 impurities, respectively. Indeed, no electronic transition is calculated for the PcLi model system at those energies.

(ii) The absorption band at 1.53 eV can be correlated with the electronic HOMO ($2a_{1u}$) \rightarrow LUMO ($6e_g^*$) transition which has a (corrected) calculated energy of 1.62 eV. This band therefore corresponds to the *Q* band observed in PcH_2 but it is not split and is shifted to lower energies due to the stabilization of the LUMO level.

(iii) The absorption band at 2.62 eV comes from the close-lying electronic transitions $5e_g \rightarrow 2a_{1u}$ and $4e_g \rightarrow 2a_{1u}$ and the band at 2.90 eV originates in the $3e_g \rightarrow 2a_{1u}$ transition. These two bands were not present in PcH_2 because they imply the promotion of an electron to the half-filled HOMO level which is doubly occupied for PcH_2 .

(iv) The band observed at 3.35 eV is attributed by Turek *et al.*³³ to the Soret or *B* band and can be correlated with the electronic transitions to the $6e_g^*$ LUMO located about 3.9–4.1 eV (see Table I). Although as for PcH_2 , the energy of this band is overestimated by the VEH calculations, the red shift predicted by the VEH method with respect to the corresponding transitions of PcH_2 (4.1–4.6 eV) is in very good accord with the bathochromic shift observed experimentally. This bathochromic shift is also observed when comparing the *B* band of the cation radical and the neutral species of Cr(III) and Fe(III) phthalocyanines.³⁴

Our assignment only differs from that reported by Turek *et al.*³³ in what concerns the bands at 1.53 and 2.62 eV. Following the general discussion reported by Minor *et al.*³⁴ for the electronic spectra of different oxidation states of metal phthalocyanines, Turek *et al.*³³ propose a *blue shift* of the *Q* band of PcLi with respect to $\text{Pc}(2-)$ compounds and assign this band to the absorption peak at 2.6 eV, while the peak at 1.53 eV is correlated with the $e_g \rightarrow 2a_{1u}$ transitions. On the contrary, Homborg *et al.*^{35,36} suggest a shift to *lower energies* for the *Q* band on the basis of the absorption spectra obtained for $\text{Pc}(-)\text{MgCl}$ ³⁵ and $\text{Pc}(-)\text{Li}$ ³⁶; this is more in the line of our own interpretations.

III. DIMERIC COMPOUNDS: METAL-FREE PHTHALOCYANINE DIMER AND LUTETIUM DIPHthalOCYANINE

The dimer of PcH_2 has been built by stacking two planar D_{2h} rings of metal-free phthalocyanine along the *z* axis. The interring distance (3.32 Å) and the ring–ring staggering angle (36.6°) assumed for the theoretical calculations are those

reported by Ciliberto *et al.*³⁷ for a silicon phthalocyanine dimer for which structural, photoelectronic, and optical data are available.^{37,38} For Pc_2Lu , the x-ray crystallographic molecular structure obtained by De Cian *et al.*³⁹ has been used for the VEH calculations. In this structure, each ring is rotated by 45° with respect to the other and both rings are severely distorted from planarity. The mean separation between the planes formed by the four isoindole nitrogens of both macrocycles is only 2.69 Å. Calculations have been performed on the Pc_2^{3-} radical again without taking into account explicitly the lutetium atom.

The one-electron energy level distribution obtained for $(\text{PcH}_2)_2$ and the Pc_2Lu model system are displayed in Fig. 3. The HOMO level corresponds to the orbital number 186 which is occupied by only one electron in the case of the Pc_2Lu radical. An overall splitting of the molecular orbitals is observed when passing from monomeric (Fig. 2) to dimeric (Fig. 3) phthalocyanines due to the interaction between both rings.

Molecular orbitals 185 and 186 (Fig. 3) result from the splitting of the $4a_u$ π -HOMO of the phthalocyanine monomer. The VEH calculations predict a splitting of 0.35 eV for $(\text{PcH}_2)_2$ in excellent agreement with the experimental values reported by Ciliberto *et al.* (0.29 eV)³⁷ and Hush *et al.* (0.32 eV)³⁸ on the basis of photoelectron spectroscopic data. A larger splitting of 0.83 eV is calculated for the Pc_2Lu model as a consequence of the closer interaction that takes place between the phthalocyanine rings in this compound. Although there are no photoemission data for Pc_2Lu , the calculated splitting is in very good accord with the absorption band observed at 0.90 eV in the near infrared electronic spectra of Pc_2Lu in dichloromethane solution.⁴⁰

The doubling of the molecular orbitals in $(\text{PcH}_2)_2$ and Pc_2Lu give rise to a great number of allowed electronic transitions. Table II summarizes the most significant among the transitions below 4 eV. It must be borne in mind that the transition energies are obtained in the same way as for PcH_2 ,

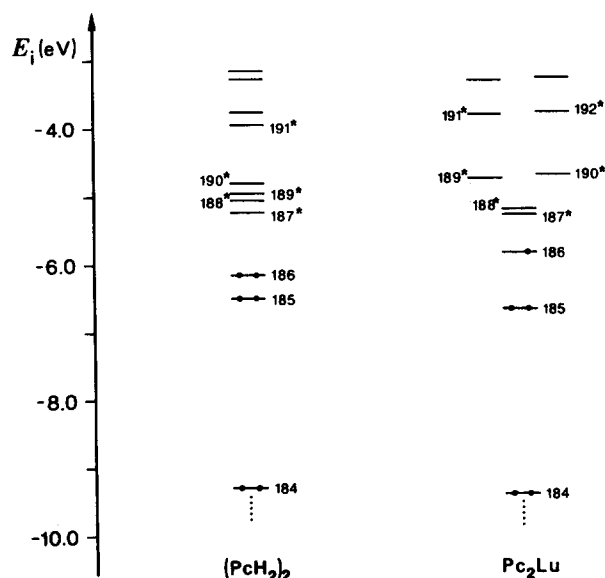


FIG. 3. VEH one-electron energies (E_i) of the upper occupied and lower unoccupied molecular orbitals calculated for $(\text{PcH}_2)_2$ and the Pc_2Lu model system. All the orbitals are of π type.

i.e., after contracting the occupied levels by a factor of 1.3 and shifting the unoccupied levels by 0.59 eV to higher energies.

The lower energy transition in Table II corresponds to the promotion of an electron from the MO number 185 to the half-occupied HOMO in Pc_2Lu . This transition has an energy of 0.83 eV and, as mentioned above, correlates very well with the first near infrared band experimentally observed for Pc_2Lu at 0.90 eV.⁴⁰ This band is polarized along the z axis and can be considered as an intramolecular charge transfer between the two phthalocyanine rings. The Pc_2Lu model molecule presents another absorption band in the near infrared region at 1.37 eV.⁴⁰ Markovitsi *et al.* assign this band to the promotion of a deeper electron to the HOMO level.⁴⁰ Our calculations, however, predict these electrons to be too low in energy and only the rather weak (oscillator strength ≈ 0.2) $186 \rightarrow 187^*$, 188^* HOMO-LUMO transitions located around 1.20 eV can be correlated with that experimental band. These two infrared bands are not obtained for $(\text{PcH}_2)_2$ since the HOMO is doubly occupied and the HOMO-LUMO gap is larger than in Pc_2Lu .

$(\text{PcH}_2)_2$ shows two rather weak transitions at energies lower than 1.7 eV (see Table II). These transitions correspond to the $186 \rightarrow 187^*$, 188^* HOMO-LUMO excitations and can be correlated with the shoulders observed on the lower energy side of the main Q band peak of silicon phthalocyanine dimers.⁴¹ The lower energy transition ($186 \rightarrow 187^*$) is calculated at 1.50 eV, 0.31 eV lower in energy than the corresponding HOMO-LUMO excitation of the PcH_2 monomer (1.81 eV). The bathochromic shift observed for this transition on going from the monomer to the dimer results from the splitting of the a_u and e_g levels which determines a narrowing of the HOMO-LUMO energy gap. This shift to

the red is not clearly seen from the optical spectra⁴¹ due to the low intensity of the $186 \rightarrow 187^*$ transition but it is in perfect agreement with experimental electrochemical data.^{42,43} Since oxidation involves removing an electron from the HOMO and reduction adding an electron to the LUMO, it is reasonable to expect a direct connection between experimental redox potentials and HOMO and LUMO energies, provided electron correlation effects do not play a major role. Cyclic voltammetry data (vs SCE) for silicon phthalocyanine compounds⁴² predict oxidation potentials of 1.00 and 0.71 V for the $\text{PcSi}(\text{OR})_2$ monomer and the $\text{RO}(\text{PcSiO})_2$ R dimer, respectively, and reduction potentials of -0.90 and -0.81 V. Two important facts are to be stressed in relation to these data. First, the 1.90 V gap measured between the oxidation and reduction potentials of the monomer fits very well with the HOMO-LUMO energy gap (1.81 eV) calculated and experimentally measured for the monomer. Second, the oxidation-reduction gap decreases by 0.38 V on going from the monomer (1.90 V) to the dimer (1.52 V) corroborating the bathochromic shift (0.31 eV) predicted by the VEH calculations for the lower energy HOMO-LUMO transition which has an energy of 1.50 eV for the $(\text{PcH}_2)_2$ dimer.

Similar sets of four intense transitions are obtained both for $(\text{PcH}_2)_2$ and the Pc_2Lu model system in the range from 1.7 to 2.1 eV (see Table II). These transitions correspond to the $186 \rightarrow 189^*$, 190^* , and $185 \rightarrow 187^*$, 188^* excitations and clearly correlate with the strong absorption Q band observed for the monomers. The complexity of this band results from the doubling of the HOMO and LUMO levels when passing from the monomer to the dimer and is in very good agreement with the multiplex structures displayed in the 600–700 nm region by metal-free phthalocyanine dimers.⁴⁴ For example, the dimer involving two phthalocyanine units linked via a benzene ring by a $-\text{OCH}_2\text{C}(\text{Me})(\text{Et})\text{CH}_2\text{O}$ group presents a broad Q band in toluene/ethanol solution with absorption peaks at 708, 673, 641, and 620 nm at room temperature. The positions of these peaks are in perfect accord with the four theoretical transitions calculated for $(\text{PcH}_2)_2$ and located at 700, 667, 646, and 611 nm (see Table II). For Pc_2Lu , the four transitions are almost degenerate two by two (transitions centered at 1.71 and 2.02 eV). However, only one absorption band is observed in the experimental spectra at an energy of 1.88 eV.^{40,45} This energy corresponds almost exactly to the center of gravity of the theoretical transitions (1.87 eV). The reduced form of Pc_2Lu (Pc_2Lu^-) displays a double absorption band at 1.77 and 2.00 eV, in very good correlation with the theoretical results.

Pc_2Lu presents another absorption band in the visible region at 2.70 eV.^{40,45} As in PcLi , this band can be attributed to electronic transitions from deeper levels to the half-occupied HOMO. A large set of these transitions is calculated between 2.70 and 2.98 eV, the maximum oscillator strength being found at 2.80 eV in good agreement with the experimental data. Finally, the Soret band (observed about 3.75 eV for $(\text{PcH}_2)_2$ ^{30,44} and 3.92 eV for Pc_2Lu ^{40,45}) can be correlated with the theoretical transitions starting at ≈ 3.9 eV with the $184 \rightarrow 187^*$ transition for both $(\text{PcH}_2)_2$ and Pc_2Lu .

The calculations performed without taking explicitly

TABLE II. VEH electronic transitions calculated for $(\text{PcH}_2)_2$ and the Pc_2Lu model system. Transitions more energetic than 4 eV or with oscillator strengths lower than 0.5 are not included. Energies are in eV (nm in parentheses).

| | Transition | Energy ^a | Oscillator strength | Polarization ^b |
|------------------------|-------------------------|------------------------|---------------------|---------------------------|
| $(\text{PcH}_2)_2$ | $186 \rightarrow 187^*$ | 1.50(827) | 1.2 | x |
| | $186 \rightarrow 188^*$ | 1.67(742) | 0.5 | y |
| | $186 \rightarrow 189^*$ | 1.77(700) | 4.8 | y |
| | $185 \rightarrow 187^*$ | 1.86(667) | 4.7 | y |
| | $186 \rightarrow 190^*$ | 1.92(646) | 4.4 | x |
| | $185 \rightarrow 188^*$ | 2.03(611) | 4.5 | x |
| | $185 \rightarrow 190^*$ | 2.28(544) | 1.1 | y |
| | $184 \rightarrow 187^*$ | 3.94(315) | 1.4 | x |
| Pc_2Lu | $185 \rightarrow 186$ | 0.83(1494) | 3.0 | z |
| | $186 \rightarrow 189^*$ | 1.69(734) | 3.6 | x,y |
| | $186 \rightarrow 190^*$ | 1.72(721) | 3.4 | x,y |
| | $185 \rightarrow 187^*$ | 1.98(626) | 3.4 | x,y |
| | $185 \rightarrow 188^*$ | 2.06(602) | 3.4 | x,y |
| | $178 \rightarrow 186$ | 2.80(443) ^c | 1.1 | x,y |
| | $184 \rightarrow 187^*$ | 3.89(319) | 0.6 | x,y |

^a Transition energies are calculated as one-electron energy differences after a contraction of 1.3 of the occupied levels and a shift of 0.59 eV to higher energies of the unoccupied levels. (See the text for further details).

^b Axes refer to those presented in Fig. 1.

^c This transition is the most intense of a group starting at 2.74 eV.

into account the lutetium atom are thus in good agreement with the Pc_2Lu optical spectrum in dichloromethane solution presented in Fig. 4. We can conclude from this result that the role of the metal electronic structure is not of prime importance in the diphthalocyanine electronic structure; this is confirmed by the fact that the Pc_2Lu (closed-shell $4f^{14}\text{Lu}^{3+}$ cation) and Pc_2Y ($3d^{10}4s^24p^6\text{Y}^{3+}$ cation) optical spectra present absorption bands located at the same energies in the visible⁴⁵ and near infrared⁴⁶ domains. The common parameter for these two metals is their ionic radius (0.93 Å) which governs the distance between the two macrocycles and, as a result, the overlap of the π orbitals. A similar conclusion can be drawn from the observation of the near-IR absorption band evolution in the series of the closely-related sandwich-like lanthanoid octaethylporphyrinate dimer complexes.⁴⁷ This band undergoes a bathochromic shift as the atomic number of the metal increases, which is simply rationalized by the parallel decrease in ionic radius of the lanthanoid ($3+$) cation. These features fully justify the approach we have followed for these calculations since the role of the metal is fairly well represented simply by its influence on the distance between the two phthalocyanine rings.

The spectrum of a Pc_2Lu film (Fig. 4) shows an additional band at 0.6 eV with respect to the spectrum recorded in solution. This band has no correspondence in the theoretical calculations for an isolated Pc_2Lu molecule. However, it is currently generally believed that this band cannot be attributed to an *intramolecular* charge transfer between the two phthalocyanine rings but rather corresponds to an *intermolecular* process.⁴⁸ Its nature will be discussed elsewhere.⁴⁶

IV. LITHIUM PHTHALOCYANINE CRYSTAL

VEH band structure calculations for the PcLi crystal have been performed based on the crystalline structure reported by Sugimoto *et al.*³² In this crystal, the phthalocyanine rings are stacked face to face along the crystalline c axis at an interplanar distance of 3.245 Å. An approximate staggering angle of 40° has been used for adjacent rings instead of the reported value of 38.7° . Again, the lithium atom is not explicitly included in the calculation.

The VEH electronic band structure calculated on the model for the PcLi crystal along the c stacking axis is schematically depicted in Fig. 5. This structure shows the same main features than those previously observed for doped

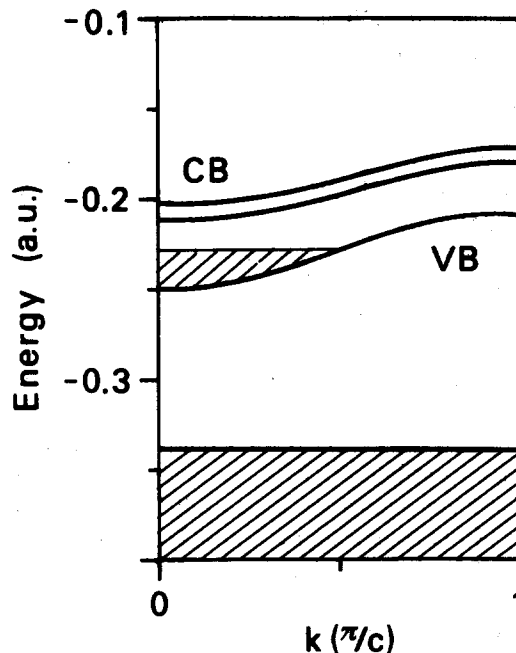


FIG. 5. VEH band structure calculated on a model PcLi crystal along the c stacking axis. VB and CB denote valence and conduction bands, respectively. VB is only half-filled.

phthalocyanine crystals.⁴⁹ The valence band lies alone well above the remaining 92 occupied bands below -8.0 eV (i.e., -0.3 atomic units of energy) and originates in the overlap of the $2a_{1u}$ (assuming a D_{4h} symmetry) π orbitals of the lithium phthalocyanine monomers. This band is only half-filled due to the single occupancy of the $2a_{1u}$ HOMO. The conduction band is formed by two nearly degenerate bands running parallel and resulting from the overlap of the $6e_g^*$ molecular orbitals. These bands would actually be degenerate in a true D_{4h} symmetry.

Valence and conduction bands are calculated to be rather broad, allowing for a good electron delocalization along the stacking axis. The width obtained for the valence band (1.08 eV) is in very good agreement with the ≈ 1 eV estimate of André *et al.*⁵⁰ on the basis of spin dynamics measurements. Since this band is only half-filled, there is no energy gap for electrical conduction along the stacking axis. Turek *et al.*¹⁰ reported a very small activation energy of 0.2 eV for electrical conduction which can be due to crystalline defects (or coulombic repulsion between conduction electrons). A total width of 0.99 eV is obtained for the almost degenerate conduction bands.

The first optical absorption corresponds to the intraband transition within the half-filled upper occupied band. The first direct interband transition is predicted to occur at $k = \pi/2c$ with an energy value of 1.50 eV. This value correlates very well with the absorption band measured at 806 nm (1.54 eV) for the PcLi crystal.³⁶ The absorption spectrum of the PcLi crystal presents the same pattern as that observed for the PcLi parent molecule and an assignment of the absorption bands similar to that discussed above for the PcLi molecule can therefore be expected. The spectrum shows an additional absorption peak at 720 nm (1.72 eV) that can be

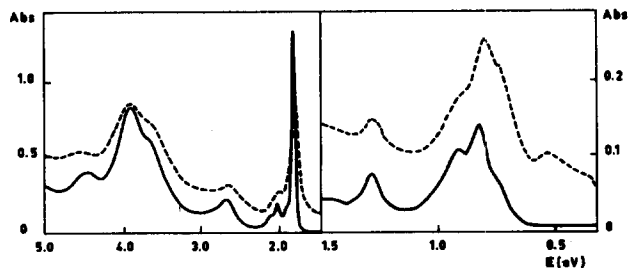


FIG. 4. Optical absorption spectra of lutetium diphthalocyanine: (i) in dichloromethane solution (solid line); and (ii) as a thin film sublimed on a quartz slide (dashed line). Note that there is a modification in the intensity scale when going from the uv-visible region to the IR region.

correlated with the $VB \rightarrow CB$ electronic transition at $k = 0$ which has an energy of 1.65 eV.

V. SYNOPSIS

We have investigated the electronic structure of five phthalocyanine compounds using the valence effective Hamiltonian nonempirical technique. In the lithium and lutetium phthalocyanines, the metal atoms are not explicitly included in the calculations. Their role can indeed be simply taken into account by employing the corresponding experimental geometries and considering the proper number of electrons of the phthalocyanine rings. The optical transitions have been calculated with the VEH method; we emphasize again that the bare optical transition values are adjusted by using a contraction (by a factor of 1.3) of the energy scale for the occupied levels and a 0.59 eV shift to higher energies of all the unoccupied levels. The lowest optical transitions obtained on that basis are found to be in excellent agreement with the experimental data.

In the monomeric systems, the lower first optical transition observed in $PcLi$ with respect to PcH_2 is due to a slight stabilization of the first unoccupied level. The origin of the Soret or B band is far more complex than what would be expected from the four-orbital model proposed by Gouterman and co-workers on the basis of the porphine electronic structure. The inadequacy of this model for phthalocyanines is related to the marked difference in the locations of the upper two occupied levels between phthalocyanine and porphine.

In the dimers, there occurs a splitting of the phthalocyanine ring energy levels. The splitting of the HOMO level for the metal-free compound is on the order of 0.35 eV, in very good agreement with the UPS data. In lutetium diphthalocyanine, the splitting is almost three times as large because the separation between the phthalocyanine rings has strongly decreased by 0.63 Å. It corresponds to the first optical transition observed at 0.9 eV due to the single occupation of the HOMO level. It is interesting to note that an additional transition at 0.6 eV is measured in phthalocyanine lutetium films. This transition is not seen in solution and is not predicted by the VEH calculations on the dimer. It is therefore interesting to note that this additional absorption is up to now attributed to an intermolecular charge-transfer transition between two dimers.

ACKNOWLEDGMENTS

We thank the University of Mons Computer Center for use of the CCI facility and FNRS, FNDP-Namur, and IBM-Belgium for use of the SCF facility. One of us (E. O.) is grateful to the University of Mons for financial support during his stay in Belgium. This work has been partly supported by CNET Lannion, the DGICYT Project PS88-0112, and the Project No. 683.2/89 from the University of Valencia.

¹For a recent review, see J. Simon and J.-J. André, *Molecular Semiconductors* (Springer, Berlin, 1985), Chap. III.

²A. T. Vartanyan, *Zh. Fiz. Khim.* **22**, 769 (1948).

³For a recent review on phthalocyanine applications, see, for example, A.

B. P. Lever, M. R. Hempstead, C. C. Leznoff, W. Lin, M. Melnik, W. A. Nevin, and P. Seymour, *Pure Appl. Chem.* **58**, 1467 (1986); R. A. Collins and K. A. Mohammed, *J. Phys. D* **21**, 154 (1988).

⁴For a review, see B. M. Hoffman and J. A. Ibers, *Acc. Chem. Res.* **16**, 15 (1983); T. J. Marks, *Science* **227**, 881 (1985); S. M. Palmer, J. L. Stanton, J. Martinsen, M. Y. Ogawa, W. B. Heuer, S. E. Van Wallendael, B. M. Hoffman, and J. A. Ibers, *Mol. Cryst. Liq. Cryst.* **125**, 1 (1985).

⁵F. Gutmann and L. E. Lyons, *Organic Semiconductors* (Wiley, New York, 1967); H. Meier, *Organic Semiconductors* (Verlag Chemie, Weinheim, 1974).

⁶E. Ortí and J. L. Brédas, *J. Chem. Phys.* **89**, 1009 (1988).

⁷J. Berkowitz, *J. Chem. Phys.* **70**, 2819 (1979).

⁸H. Höchst, A. Goldmann, S. Hüfner, and H. Malter, *Phys. Status Solidi B* **76**, 559 (1976); F. L. Battye, A. Goldmann, and L. Kasper, *ibid.* **80**, 425 (1977); E. Tegeler, M. Iwan, and E.-E. Koch, *J. Electron. Spectrosc. Relat. Phenom.* **22**, 297 (1981).

⁹M. Maitrot, G. Guillaud, B. Boudjema, J.-J. André, H. Strzelecka, J. Simon, and R. Even, *Chem. Phys. Lett.* **133**, 59 (1987).

¹⁰Ph. Turek, P. Petit, J.-J. André, J. Simon, R. Even, B. Boudjema, G. Guillaud, and M. Maitrot, *J. Am. Chem. Soc.* **109**, 5119 (1987).

¹¹Ph. Turek, P. Petit, J.-J. André, J. Simon, R. Even, B. Boudjema, G. Guillaud, and M. Maitrot, *Mol. Cryst. Liq. Cryst.* **161**, 323 (1988).

¹²J. Simon, F. Tournilhac, and J.-J. André, *Nouv. J. Chim.* **11**, 383 (1987).

¹³P. Petit, K. Holczer, and J.-J. André, *J. Phys.* **48**, 1363 (1987).

¹⁴N. N. Usov and V. A. Benderskii, *Phys. Status Solidi B* **37**, 535 (1970); G. A. Cox and P. C. Knight, *J. Phys. Chem. Solids* **34**, 1655 (1973).

¹⁵C. Hamann, M. Starke, and H. Wagner, *Phys. Status Solidi A* **16**, 463 (1973).

¹⁶C. Hamann and I. Storbeck, *Naturwissenschaften* **50**, 327 (1963).

¹⁷G. Nicolas and Ph. Durand, *J. Chem. Phys.* **70**, 2020 (1979); **72**, 453 (1980).

¹⁸J. M. André, L. A. Burke, J. Delhalle, G. Nicolas, and Ph. Durand, *Int. J. Quantum Chem. Symp.* **13**, 283 (1979).

¹⁹J. L. Brédas, R. R. Chance, R. Silbey, G. Nicolas, and Ph. Durand, *J. Chem. Phys.* **75**, 255 (1981).

²⁰B. Thémans, J. M. André, and J. L. Brédas (unpublished).

²¹J. L. Brédas, B. Thémans, and J. M. André, *J. Chem. Phys.* **78**, 6137 (1983).

²²B. F. Hoskins, S. A. Mason, and J. C. B. White, *J. Chem. Soc. Chem. Commun.* **1969**, 554.

²³A. Henriksson and M. Sundbom, *Theor. Chim. Acta* **27**, 213 (1972).

²⁴L. K. Lee, N. H. Sabelli, and P. R. LeBreton, *J. Phys. Chem.* **86**, 3926 (1982).

²⁵A. M. Schaffer and M. Gouterman, *Theor. Chim. Acta* **25**, 62 (1972).

²⁶Z. Berkovitch-Yellin and D. E. Ellis, *J. Am. Chem. Soc.* **103**, 6066 (1981).

²⁷L. Edwards and M. Gouterman, *J. Mol. Spectrosc.* **33**, 292 (1970).

²⁸E. Ortí, M. C. Piqueras, R. Crespo, and J. L. Brédas, *Chem. Materials* (in press).

²⁹C. Weiss, H. Kobayashi, and M. Gouterman, *J. Mol. Spectrosc.* **16**, 415 (1965).

³⁰K. A. Martin and M. J. Stillman, *Can. J. Chem.* **57**, 1111 (1979).

³¹E. Ortí and J. L. Brédas, *Chem. Phys. Lett.* (in press).

³²H. Sugimoto, M. Mori, H. Masuda, and T. Taga, *J. Chem. Soc. Chem. Commun.* **1986**, 962.

³³Ph. Turek, J.-J. André, A. Giraudeau, and J. Simon, *Chem. Phys. Lett.* **134**, 471 (1987).

³⁴P. C. Minor, M. Gouterman, and A. B. P. Lever, *Inorg. Chem.* **24**, 1894 (1985).

³⁵H. Homborg, *Z. Anorg. Allg. Chem.* **507**, 35 (1983).

³⁶H. Homborg and C. L. Teske, *Z. Anorg. Allg. Chem.* **527**, 45 (1985).

³⁷E. Ciliberto, K. A. Doris, W. J. Pietro, G. M. Reisner, D. E. Ellis, I. Fragalà, F. H. Herbstein, M. A. Ratner, and T. J. Marks, *J. Am. Chem. Soc.* **106**, 7748 (1984).

³⁸N. S. Hush and A. S. Cheung, *Chem. Phys. Lett.* **47**, 1 (1977).

³⁹A. De Cian, M. Moussavi, J. Fischer, and R. Weiss, *Inorg. Chem.* **24**, 3162 (1985).

⁴⁰D. Markovitsi, T.-H. Tran-Thi, R. Even, and J. Simon, *Chem. Phys. Lett.* **137**, 107 (1987).

⁴¹N. S. Hush and I. S. Woolsey, *Mol. Phys.* **21**, 465 (1971).

⁴²B. L. Wheeler, G. Nagasubramanian, A. J. Bard, L. A. Schechtman, D. R. Dininny, and M. E. Kenney, *J. Am. Chem. Soc.* **106**, 7404 (1984).

⁴³T. M. Mezza, N. R. Armstrong, G. W. Ritter II, J. P. Iafelice, and M. E. Kenney, *J. Electroanal. Chem. Interfacial Electrochem.* **137**, 227 (1982).

⁴⁴E. S. Dodsworth, A. B. P. Lever, P. Seymour, and C. C. Leznoff, *J. Phys.*

- Chem. **89**, 5698 (1985).
- ⁴⁵C. Clarisse and M. T. Riou, *Inorg. Chim. Acta* **130**, 139 (1987).
- ⁴⁶M. T. Riou and C. Clarisse (unpublished).
- ⁴⁷J. W. Buchler and B. Scharbert, *J. Am. Chem. Soc.* **110**, 4272 (1988).
- ⁴⁸R. Even, J. Simon, and D. Markovitsi, *Chem. Phys. Lett.* **156**, 609 (1989).
- ⁴⁹E. Ortí and J. L. Brédas, *Synth. Met.* **29**, F115 (1989).
- ⁵⁰J. J. André, K. Holczer, P. Petit, M.-T. Riou, C. Clarisse, R. Even, M. Fourmigué, and J. Simon, *Chem. Phys. Lett.* **115**, 463 (1985).